Atmos. Chem. Phys. Discuss., doi:10.5194/acp-2016-23, 2016
Manuscript under review for journal Atmos. Chem. Phys.
Published: 25 January 2016

Atmospheric Chemistry and Physics Discussions

Variation of CCN activity during new particle formation events in the North China Plain

N. Ma[1,2,4], C. S. Zhao[2,*], J. C. Tao[2], Z. J. Wu[3], S. Kecorius[1], Z. B. Wang[1,4], J. Größ[1], H. J. Liu[2], Y. X. Bian[2], Y. Kuang[2], M. Teich[1], G. Spindler[1], K. Müller[1], D. van Pinxteren[1], H. Herrmann[1], M. Hu[3], A. Wiedensohler[1]

[1]Leibniz Institute for Tropospheric Research, Leipzig 04318, Germany
[2]Department of Atmospheric and Oceanic Sciences, School of Physics, Peking University, Beijing 100871, China
[3]College of Environmental Sciences and Engineering, Peking University, Beijing 100871, China
[4]Multiphase Chemistry Department, Max Planck Institute for Chemistry, Mainz 55128, Germany

Correspondence to: C. S. Zhao (zcs@pku.edu.cn)

Abstract. The aim of this investigation was to obtain a better understanding of the variability of the cloud condensation nuclei (CCN) activity during new particle formation (NPF) events in an anthropogenically polluted atmosphere of the North China Plain (NCP). We investigated the size-resolved activation ratio as well as particle number size distribution, hygroscopicity and chemical composition during an intensive field experiment at a regional atmospheric observatory at Xianghe. Interestingly, two types of NPF events were found, in which the growth of the newly formed particles is dominated by either sulfate or organic matters. The particle CCN activity therefore significantly differs in those NPF events, indicating that it might be difficult to find a simple parameterization of particle CCN activity during NPF events over the NCP. For an accurate estimation of the potential CCN number concentration (N_{CCN}) during NPF events, the variation of CCN activity has to be taken into account. Considering that a fixed activation ratio curve or critical diameter are usually used to calculate N_{CCN}, the influence of the variation of particle CCN activity on the calculation of N_{CCN} during NPF events was evaluated based on these two parameterizations. It was found that N_{CCN} might be underestimated by up to 30% if a fix activation ratio curve (representative of the region and season) is used in the calculation; and might be underestimated by up to 50% if a fix critical diameter (representative of the region and season) is used. Therefore, we suggest not using a fixed critical diameter in the prediction of N_{CCN} in NPF seasons. If real-time CCN activity data is not available, using a proper fixed activation ratio curve can be a compromising choice.

Atmos. Chem. Phys. Discuss., doi:10.5194/acp-2016-23, 2016
Manuscript under review for journal Atmos. Chem. Phys.
Published: 25 January 2016

Atmospheric Chemistry and Physics Discussions

1 Introduction

Atmospheric nucleation and the subsequent particle growth of nucleated clusters (new particle formation event, NPF event) is frequently observed in a variety of environments around the world (Kulmala et al., 2004; Kulmala and Kerminen, 2008 and references therein), which is believed to be an important source of cloud condensation nuclei (CCN). However, the contribution of homogeneous nucleation to the CCN number concentration is still not well defined, therefore gained a lot of attentions during the last decade (Kerminen et al., 2012 and references therein).

Because the size of a particle plays the most important role in determining its CCN activity (Dusek et al., 2006), many studies used the number concentration of particles larger than a distinct diameter (integral of particle number size distribution, PNSD) as a proxy of the number concentration of potential CCN for a certain super saturation (SS). This method yields into an average relative contribution of NPF spanning from few percent to several tens of percent for different SS and regions (e.g. Laaksonen et al., 2005; Kuang et al., 2009; Asmi et al., 2011; Peng et al., 2014). Without a direct measurement of the CCN number concentration, such kind of treatment is reasonable to obtain a rough approximation of the contribution of NPF. However, large uncertainties might be included in those results. Only few studies investigated the variation of the CCN number concentration during the NPF event with direct CCN measurement (e.g. Kuwata et al., 2008; Wiedensohler et al., 2009; Sihto et al., 2011).

The diameter of nucleated clusters is around 1 – 2 nm (Kulmala et al., 2007). To contribute to the CCN number concentration, newly formed particles need to grow about 10^5 times in volume (i.e. at least up to 50 nm). This means that the chemical composition of those particles is basically determined by the condensing material. Although not as important as size, particle chemical composition also plays some roles in determining its CCN activity. A number of studies investigated the mechanism of the growth of newly formed particles. Low-volatile organic compounds are suggested to play the major role in particle growth (Kulmala et al., 1998; Kerminen et al., 2000, Wehner et al., 2005), which has been proved in many observations in different region (e.g. Laaksonen et al., 2008; Smith et al., 2010; Ehn et al., 2014); while sulfuric acid was also found to play an important role in the growth process (Birmili et al., 2003; Boy et al., 2005). Yue et al. (2010) found two types of NPF events in Beijing in which either sulfate or organic matters (OM) can be the dominant species in ultrafine particles. Therefore, the CCN activity of newly formed particles may differ in different regions and cases, depending on the dominant process in the particles growth. This means, the NPF may influence CCN budget not only by modifying particle number size distribution, but also by changing particle CCN activity. However, the variation of particle CCN activity during the NPF event was very seldom discussed in previous studies. Especially in China, no investigation was done for regional NPF events.

Measurements of aerosol particle optical properties (Ma et al., 2011, 2012), hygroscopicity (Liu et al., 2011) and CCN activation (Deng et al., 2011) during the Haze campaign in China (HaChi) showed that the North China Plain (NCP) is one of the most anthropogenically polluted regions in the world. With abundant precursors in the NCP, NPF is frequently occurred (Wu et al., 2007; Wang et al., 2013a), and has distinct contribution on the particle concentration (Guo et al., 2014).

Atmos. Chem. Phys. Discuss., doi:10.5194/acp-2016-23, 2016
Manuscript under review for journal Atmos. Chem. Phys.
Published: 25 January 2016

The high number concentration of aerosol particles in the NCP may have impacts on cloud microphysical properties and precipitation (Zhao et al., 2006a, b; Deng et al., 2009). To have a better understanding of these impacts, it is essential to have a precise parameterization of particle CCN activity in this polluted region. In the first step, we have therefore to investigate and understand the contribution and influence of NPF on particle CCN activity.

2 Measurements and data processin

2.1 Observational Site

During July 9th to August 8th in 2013, aerosol microphysical and optical properties were measured at Xianghe station (39.75 N, 116.96 E, 36 m a.s.l.), a regional atmospheric observatory in the NCP about 50 km southeast from Beijing and 70 km west from Tianjin (Figure 1). The observatory is located close to a small village and about 5 km west of Xianghe city center. The surroundings are farmland and residential areas. The measurements can be assumed to be representative of the regional background aerosol of the north NCP during daytime. From time to time, an influence of local anthropogenic emission could be identified during nighttime. More information about the site can be found in Zhang et al. (2016).

Most of the online instruments are located in a measurement container, in which the temperature was maintained at 22 ℃. The inlet system consisted of a PM10 inlet (Rupprecht & Patashnick Co., Inc., Thermo, 16.67 l/min), three in-line Nafion dryers (Wiedensohler et al., 2013) and an automatic absorption dryer based on the design by Tuch et al. (2009). This set up ensured a relative humidity in the aerosol sample flow below 30%. In the measurement container, sampled aerosol was fed to separate instruments through stainless steel/conductive tubing using an isokinetic flow splitter.

2.2 Particles number size distribution

A mobility particle size spectrometer (TROPOS-type scanning mobility particle size spectrometer, SMPS; Wiedensohler et al., 2012), consisting of a Hauke-type medium differential mobility analyzer (DMA, 28 cm effective length) and a condensation particle counter (CPC Model 3772; TSI, Inc., Shoreview, MN USA), was used to measure PNSDs with mobility diameter from 9 to 800 nm with temporal resolution of 5 min. The measurements were performed in compliance with recently issued guidelines for atmospheric particle size distribution measurements (Wiedensohler et al., 2012). Data evaluation includes a multiple charge correction (Pfeifer et al., 2014), counting efficiency correction of the condensation particle counters (Wiedensohler et al., 1997), and corrections for the diffusion losses in the system and inlet tubing.

2.3 Size-resolved particle activation ratio

The size-resolved particle activation ratio (AR), defined as the ratio between the number of particles which can be activated at a certain SS and the total number of particles at a certain diameter, was measured by a DMA-CCNC system. The system consists of an electrostatic classifier (Model 3080; TSI, Inc., Shoreview, MN USA), a condensation particle counter (CPC Model 3772; TSI, Inc., Shoreview, MN USA), and a continuous-flow CCN counter (Model CCN200, Droplet Measurement

Atmos. Chem. Phys. Discuss., doi:10.5194/acp-2016-23, 2016
Manuscript under review for journal Atmos. Chem. Phys.
Published: 25 January 2016

Technologies, USA; Roberts and Nenes, 2005; Lance et al., 2006). More details about the system are given in Deng et al. (2011). The sample flow of the DMA was split into two flows with flow rate of 1.0 l/min and 0.5 l/min. The CPC and CCN counter measured then the total particle and the CCN number concentration for a certain particle size.

During the measurement, the SS in the CCN counter was circularly set to five values, with 20 min for 0.07% and 10 min each for 0.10%, 0.20%, 0.40% and 0.80%. Two complete size scans were covered in the duration of each SS (4 scans for 0.07%), and only the last scan during each supersaturation was used since the system needs some time for stabilizing the temperature in the column after changing the SS. The data from CCN counter during the selected period was matched with particle number concentration measured by the CPC. The size-resolved particle activation ratio was then inverted using a modified algorithm based on Hagen and Alofs (1983) (Deng et al., 2011). Finally, the size-resolved activation ratios were available for all the 5 SS in each hour. The sheath and sample flow rates, as well as the SS of CCN counter were calibrated before the campaign and check at the end of the campaign (Rose et al., 2008).

To have a better insight into the temporal variation of CCN activity, the diameter of 50% activation ratio ($D_{P,50}$) and the slope of activation ratio curve (S_{50}) were used. S_{50} was calculated as $\frac{0.2}{\log D_{P,60} - \log D_{P,40}}$, where $D_{P,40}$ and $D_{P,60}$ are the diameter of 40% and 60% activation ratio, respectively.

2.4 Particle hygroscopicity

Particle hygroscopic growth factor (f_g), defined as the ratio between the particle diameter at a certain relative humidity (RH) and the particle dry diameter, was measured with a hygroscopic tandem differential mobility analyzer (TROPOS-type HTDMA; Massling et al., 2007) at 87% RH for dry diameters ($D_{P,dry}$) of 50, 100, 150, 200, 250, 350 nm. The time resolution of the full scan covering all the 6 sizes was about 50 min. The probability density function of f_g (f_g-PDF) is obtained based on the measured distribution function of f_g with TDMAinv algorithm developed by Gysel et al. (2009). Calibration with ammonium sulfate particles was automatically conducted every 6 hours.

A hygroscopicity parameter κ was calculated according to Petters et al. (2007):

$$\kappa = \left(f_g^3 - 1\right) \cdot \left(\frac{1}{S}\exp\left(\frac{4\sigma_{s/a} M_W}{RT\rho_W D_{P,dry} f_g}\right) - 1\right) \quad (1)$$

where S is the saturation ratio; ρ_W is the density of water; M_W is the molecular weight of water; $\sigma_{s/a}$ is the surface tension of the solution / air interface which is assumed to be equal to the surface tension of the pure water / air interface; R is the universal gas constant; and T is the temperature. The probability density function of κ (κ-PDF) was then derived and used in this study. As shown in Zhang et al. (2016), the κ-PDF usually exhibits a bi-model or tri-model shape. In this study, we simply define the particles with $\kappa > 0.1$ as hygroscopic mode particles, and the rest as hydrophobic mode particles. More details about this measurement and data processing can be found in Zhang et al. (2016).

Atmos. Chem. Phys. Discuss., doi:10.5194/acp-2016-23, 2016
Manuscript under review for journal Atmos. Chem. Phys.
Published: 25 January 2016

2.5 Particle chemical composition

A Digitel high volume (HV) DHA-80 filter sampler (Riemer, Hausen, Germany) was used to collect atmospheric particles of an aerodynamic diameter less than 10 μm (PM10) on quartz fiber filters (MK 360, Munktell, Falun, Sweden). To reduce the blank content of carbonaceous material, the filters were heated for 24 h at 105 ℃ before sampling. After sampling the filters were stored at −20°C until usage. Samples were taken every 12 h (day time samples: 6:00 – 18:00 LT, night time samples: 18:00 LT until six on the following morning) at a flow rate of 0.5 m^3 min^{-1}.

Inorganic ions were analyzed by ion chromatography (IC690 Metrohm, Switzerland; ICS3000, Dionex, USA). Before analysis, a filter aliquot was extracted in deionized water by shaking and ultrasonication and filtered through 0.45-mm-pore-size syringe filters.

The determination of total carbon (TC) as organic carbon (OC) and elemental carbon (EC) was carried out by a thermal-optical method using the Sunset Laboratory Dual-Optical Carbonaceous Analyzer (Sunset Laboratory Inc., U.S.A.). For analyses of quartz filters the EUSAAR 2 temperature-protocol was used and a charring correction using light transmission was applied (Cavalli et al. 2010).

3 Results and discussion

3.1 New particle formation events in the NCP

NPF events were frequently observed in the north NCP. Based on a 1-year data set, Wu et al. (2007) found NPF events on 40% measurement days in an urban background station in Beijing. At the regional atmospheric observatory and regional GAW (Global Atmosphere Watch) station Shangdianzi, the frequency of NPF day was found to be 36% based on a continuously measurement longer than 1 year (Shen et al., 2011).

During our intensive field campaign, NPF events were observed during 10 out of 28 days, in which a clear growth of newly formed particles were found on 5 days. The variation of particle number size distribution, κ-PDF of 50 nm particles, and the mass fraction of organic matter and sulfate in PM10 during these 5 NPF days are shown in Figure 2. During the first NPF event occurred on July 20th, the nucleation mode did not start at the lower detection limit of our SMPS, meaning that the nucleation might have taken place upstream of our measurement site. This event was however counted as a NPF event, since the hygroscopicity and CCN activity of the nucleation mode particles during NPF event is basically determined by the growth process, which was observed on that day. It can be seen that the NPF events started in the morning on all the 5 days. In the first 3 cases, the newly formed particle kept on growing towards the end of the day. In the other 2 cases, the growth was interrupted in the afternoon.

It is interesting to note in Figure 2 that the hygroscopicity of newly formed particles is largely different in the five events. On July 20th, 22nd and 25th, after the nucleation mode reaching 50 nm, the κ-PDF at 50 nm shows a dominant hygroscopic mode at κ of around 0.4 until 18:00 LT. However, the newly formed particles show a much lower κ on July 24th and 28th: in the late afternoon on July 24th, the hygroscopic mode of κ-PDF is located between 0.1 and 0.2; on July 28, the κ of hygroscopic

Atmos. Chem. Phys. Discuss., doi:10.5194/acp-2016-23, 2016
Manuscript under review for journal Atmos. Chem. Phys.
Published: 25 January 2016

mode is also lower than 0.2. The particle hygroscopicity parameter κ is mainly determined by its chemical composition (Petters and Kreidenweis, 2007). Therefore, it can be assumed that the particulate matter produced during the growth process is dominated by different species in different NPF events.

The mass fraction of organic matters and sulfate in PM10 obtained from offline analysis of 12-h DIGITEL HV-samples are shown in the bottom subplots of Figure 2. The ultrafine particles take only a minor fraction in PM10 total mass. However, the temporal variation of the mass fraction of a certain species in PM10 can to some extent indicate its production activity. It can be seen that the average mass fraction of OM in the daytime of July 20th, 22nd and 25th is lower than the average of the previous nighttime, while the mass fraction of sulfate obviously increase (July 22nd and 25th) or at least stayed at the same level (July 20th), meaning that the secondary production of sulfate is more active than that of OM. The opposite variation can be found on July 24th and 28th, meaning that the production of OM was more efficient during the growth of the newly formed particles. Considering the hygroscopicity of sulfate and OM, this result is consistent with the aforementioned variation of κ-PDF in the five events.

Our result is in agreement with Yue et al. (2010). They found that in Beijing area, condensation and neutralization of sulfuric acid contribute 45±18% to the apparent growth rate on average, and organic compounds are also an important contributor. And two types of NPF events were observed in which the growth process is driven by either organics or sulfates.

3.2 Variation of CCN activity during the NPF events

Newly formed particles may grow up to CCN-active sizes in few hours and contribute to the total CCN number concentration (e.g. Wiedensohler et al., 2009; Yue et al., 2011; Wang et al., 2013b; Wu et al., 2015). As discussed above, the hygroscopicity and chemical composition of aerosol particles differs in different NPF events in the NCP. The CCN activity of aerosol particles and the CCN productivity of NPF might therefore also differ in different events. The NPF events on July 22nd and 24th are selected and discussed in detail in this section. Considering the variation of the particle hygroscopicity and the mass fraction of sulfate and OM, we name the two events as sulfate-dominant NPF event and OM-dominant NPF event, respectively.

3.2.1 CCN activity in sulfate-dominant NPF event

Figure 3 illustrates the NPF event occurred on July 22nd. July 22nd is a hazy day with the average temperature, RH and wind speed of 26.1 ℃, 77.5% and 0.4 ms^{-1}, respectively. The weak south-southwest wind starting from the previous day facilitates the accumulation of pollutants in the region (Xu et al., 2011). The daily average BC mass concentration is 6.94 μgm^{-3}, higher than the average of the entire measurement period (4.66 μgm^{-3}).

As the developing of the boundary layer in the morning, the BC mass concentration and particle condensational sink (CS, Kulmala et al., 2001) start to decrease at 07:00 LT. The newly formed particles start to be visible in our SMPS record at around 09:00 LT, and keep on growing until the end of the day with an average growth rate of 6.3 nm h^{-1} (Figure 3A). The newly formed particles reach 50 nm at around 10:30 LT, resulting in a sharp elevation of $N_{[40\text{-}60nm]}$ from about 2×10^3 cm^{-3} to

Atmos. Chem. Phys. Discuss., doi:10.5194/acp-2016-23, 2016
Manuscript under review for journal Atmos. Chem. Phys.
Published: 25 January 2016

Atmospheric Chemistry and Physics Discussions

1×10^4 cm^{-3}. Correspondingly, the average κ of hygroscopic mode particles ($\kappa_{ave,H}$) increase from around 0.3 to 0.45 within 1 hour (Figure 3D). Since the newly formed particles grow up to 50 nm and become the majority, the number fraction of hydrophobic mode particles (NF_{NH}) decreases from about 0.2 to 0. Such a great variation in particle hygroscopicity indicates that the chemical composition of 50 nm particles during the NPF event is different from that of pre-existing ones.

The mass concentration and fraction of the major compounds in PM10 is shown in Figure 4. As mentioned in section 3.1, the ultrafine particles only take a minor fraction in PM10 total mass. However, the temporal variation of the mass fraction of different chemical compounds may provide some information about the secondary aerosol production. We can see that SO_4^{2-} takes 21.5% of PM10 total mass concentration on average during the daytime of July 22nd (11:00 LT – 17:52 LT), which is almost double of that for the night before (July 21st 18:55 LT – July 22nd 06:55 LT). This indicates that the secondary production of sulfate is very active during that period, and makes a major contribution on the PM10 mass. Considering the high hygroscopicity of the newly formed particles (average κ about 0.45), it is reasonable to assume that sulfate takes the main mass fraction in those particles.

During this NPF event, an enhancement of aerosol CCN activity can be seen. As the $N_{[40\text{-}60nm]}$ increases sharply at around 10:30 LT, $D_{P,50}$ decreases from about 46 nm to 39 nm for 0.80% SS, and decrease from about 70 nm to 60 nm for 0.40% SS (Figure 3E). The S_{50} increases from about 3.5 to 6.0 for 0.80% SS and increases from about 4 to 6 for 0.40% SS (Figure 3F), meaning that the size-resolved activation ratio curve gets steeper. It is interesting that enhancement of aerosol CCN activity can also be seen for 0.20% SS, for which $D_{P,50}$ is out of the size range dominated by the newly formed particles (Figure 3C). This is because the secondarily produced compounds may condense on all particles. The CCN activity of pre-existing particles might therefore increase.

To have a better view of particle CCN activity during the NPF event, three records of size-resolved activation ratio before and during the NPF event are selected and averaged (the corresponding records are marked as color-filled points in Figure 3E), as shown in Figure 5. The activation ratio before the nucleation is basically the same as the campaign average for all the three SS. However, the activation ratio curves obviously shift towards lower size and get steeper during the NPF event for SS of 0.40% and 0.80%, indicating that the particles are more hygroscopic, and with a narrower probability distribution of hygroscopicity compared with the pre-existing particles (Su et al., 2010).

In the nighttime after 18:00 LT, due to the collapse of the boundary layer and the increase of aerosol emission (traffic and cooking), the influence of anthropogenic emission starts to be visible in the time series of particle number size distribution (Figure 3A). The newly formed particles keep on growing largely contributed by the coagulation and condensation of the freshly emitted particulate and gaseous pollutants, and therefore become less hygroscopic. The BC mass concentration increases significantly after 18:00 LT and shows a peak of about 20 μgm^{-3} at around 22:00 LT (Figure 3B), resulting in an increase of the number fraction of hydrophobic mode particles (Figure 3D). These results indicate that in the nighttime the major particle population is getting less hygroscopic, and different compounds are inhomogeneous distributed among particles. Accordingly, particle CCN activity varies a lot in this period (Figure 3E and F). Compared with the campaign-average, the activation ratio curve in nighttime is flatter and shift towards larger size. Considering the increasing BC mass

Atmos. Chem. Phys. Discuss., doi:10.5194/acp-2016-23, 2016
Manuscript under review for journal Atmos. Chem. Phys.
Published: 25 January 2016

Atmospheric Chemistry and Physics Discussions

concentration, the BC emission is very likely to play the major role in the variation of CCN activity in nighttime. Condensation of insoluble organic compounds might be also responsible.

3.2.2 CCN activity in OM-dominant NPF event

Figure 6 displays another NPF event occurred on July 24th. This day is relatively clean with cloudless blue sky. The daily average temperature and RH is respectively 28.4 ℃ and 70.5%. The BC mass concentration stays at a low level (1.74 μgm^{-3}) in daytime due to the 2 ms^{-1} northwest wind and the development of the boundary layer.

The NPF event starts at around 09:00 LT. The newly formed particles keep on growing throughout the day with an average growth rate of 6.3 nm h^{-1} (Figure 6A). It can be seen that $N_{[40\text{-}60nm]}$ increase from about 2×10^3 cm^{-3} to 1.4×10^4 cm^{-3} in a few hours, $N_{[60\text{-}80nm]}$ also increase during the daytime. As the newly formed particles grow up to 50 nm and become the majority at this size, the number fraction of hydrophobic mode particles decreases to almost 0 within 1 hour. It is interesting to note that, unlike the event on July 22nd, the average κ for hygroscopic mode of 50 nm particles deceases a bit after the nucleation, and stays below 0.3 for the rest of the day. Such low hygroscopicity of newly formed particles implies that the driving mechanism of particle growth in daytime for this event is somehow different from the event on July 22nd. We can see in Figure 4 that the average mass fraction of SO_4^{2-} in PM10 in the daytime (July 24th 06:03 LT – 18:03 LT) is slightly lower than that in the previous night (July 23rd 18:03 LT – July 24th 06:03 LT). In contrast, the mass fraction of OC increases from 14.1% (July 23rd 18:03 LT – July 24th 06:03 LT) to 20.0% (July 24th 06:03 LT – 18:03 LT) which is nearly double the mass fraction of SO_4^{2-}. It therefore can be assumed that the condensation of low-volatile OC plays a major role in the growth of the newly formed particles in the daytime.

With the active secondary production of OC which is less hygroscopic or even hydrophobic, no enhancement can be found in particle hygroscopicity and CCN activity in daytime (Figure 6D and E). $D_{P,50}$ for 0.20% SS even increase from about 110 nm to 120 nm. The average size-resolved activation ratio for 0.20%, 0.40% and 0.80% SS at selected time (marked as color-filled points in Figure 6E) are shown in Figure 5. Different from the event on July 22nd, due to the decrease of particle hygroscopicity, the average activation ratio curves shift a bit towards larger size during the new particle formation event.

The nighttime story on July 24th is similar as on July 22nd. The increasing anthropogenic emission causes a decrease in particle hygroscopicity and CCN activity (Figure 6D, E and F). Nocturnal nucleation also occurred on July 24th (Figure 6A), which is discussed in detail in Kecorius et al. (2015).

3.3 Influence of the varying CCN activity on the CCN prediction during NPF events

One of the aims of studying particle CCN activity is to predict the CCN number concentration (N_{CCN}). Defined as the number concentration of particles which can be activated at a certain SS, N_{CCN} can be calculated as follows:

$$N_{CCN} = \int_{\log D_P} AR(\log D_P, SS)\cdot n(\log D_P)\cdot d\log D_P \quad (2)$$

Atmos. Chem. Phys. Discuss., doi:10.5194/acp-2016-23, 2016
Manuscript under review for journal Atmos. Chem. Phys.
Published: 25 January 2016

Atmospheric Chemistry and Physics Discussions

where, $n(\log D_P)$ is the particle number size distribution. It can be learned from Eq. (2) that N_{CCN} is determined by both the size-resolved activation ratio and particle number size distribution. Since CCN activity mainly depends on particle size (Dusek et al., 2006), N_{CCN} is more sensitive on the variation of particle number size distribution (Deng et al., 2013). Also direct measurement of particle CCN activity and hygroscopicity are difficult to be widely applied. Therefore, a fixed size-resolved activation ratio curve or critical diameter (normally averaged over a certain period) is usually used when evaluating the contribution of NPF on N_{CCN}. However, as discussed in Sect. 3.2, activation ratio curve can vary largely in NPF days in the NCP. Moreover, the activation ratio curve might be different in different types of NPF events. The question then arises as to can we just use an average activation ratio curve or a fixed critical diameter for NPF events, or what is the possible bias if an average activation ratio curve or a fixed critical diameter is applied.

To answer this question, N_{CCN} was calculated with eq. (2) based on campaign average activation ratio ($N_{CCN,AR\text{-}ave}$), campaign average critical diameter ($N_{CCN,D\text{-}ave}$) and real-time activation ratio ($N_{CCN,ref}$). The real-time particle number size distribution was used in the calculation. The campaign average critical diameter for a certain SS ($D_{P,cri}$) was chosen as follows: firstly, $D_{P,cri}$ was calculated for each data record by solving

$$N_{CCN,ref} = \int_{\log D_{P,cri}}^{\log D_{P,max}} n(\log D_P)\, d\log D_P \quad (3)$$

where, $D_{P,max}$ is the maximum diameter of the measured particle number size distribution; then the geometric average of $D_{P,cri}$ for the whole period was calculated and used. The calculated $D_{P,cri}$ is 55.3, 80.6 and 114.9 nm for 0.80%, 0.40% and 0.20% SS, respectively. Without direct measurement of N_{CCN}, the N_{CCN} calculated with real-time activation ratio was taken as the reference value. The relative difference between N_{CCN} calculated with campaign average activation ratio / critical diameter and the reference value during the two NPF days was then evaluated.

On July 22nd (sulfate-dominant NPF event), as the growing of the newly formed particles, N_{CCN} at 0.80% SS increase doubly during the daytime, from about 1.3×10^4 to 2.5×10^4 cm^{-3}. Since sulfate dominates the particle growth, the CCN activity of aerosol particles increases during the NPF. As shown before, the activation ratio curve got steeper and shifted towards smaller size compared with the campaign average curve. $N_{CCN,AR\text{-}ave}$ is therefore respectively about 20%, 15% and 10% lower than $N_{CCN,ref}$ for SS of 0.80%, 0.40% and 0.20% in the daytime. On July 24th (OM-dominant NPF event), since OM contributes more than sulfate on the growth of the particles, the activation ratio curve during particle growth is very similar as the campaign average (0.80% SS), or even moves a bit to the larger size in the afternoon (0.40% and 0.20% SS, Figure 6). The relative difference between $N_{CCN,AR\text{-}ave}$ and $N_{CCN,ref}$ for 0.80% SS during daytime is about -8%, which is much less than the case of July 22nd. For 0.40% and 0.20% SS, $N_{CCN,AR\text{-}ave}$ is even much higher than $N_{CCN,ref}$ in the afternoon.

When using the average $D_{P,cri}$, the calculated $N_{CCN,D\text{-}ave}$ is lower than $N_{CCN,ref}$ in both two NPF events. The relative differences between $N_{CCN,D\text{-}ave}$ and $N_{CCN,ref}$ are respectively about -40%, -30% and -10% for 0.80%, 0.40% and 0.20% SS in the afternoon of July 22nd, and -35%, -40% and 10% for the three SS in the afternoon of July 24th.

Atmos. Chem. Phys. Discuss., doi:10.5194/acp-2016-23, 2016
Manuscript under review for journal Atmos. Chem. Phys.
Published: 25 January 2016

Atmospheric Chemistry and Physics Discussions

To give a more general result, the relative difference between $N_{CCN,AR\text{-}ave}$ (and also $N_{CCN,D\text{-}ave}$) and $N_{CCN\text{-}ref}$ were calculated for the entire measurement period. Its overall frequency distribution and the frequency distribution at different time of day are shown in Figure 7.

It can be seen in Figure 7A that when using the average activation ratio, the majority of the biases in the calculated N_{CCN} are located between -0.1 and 0.1, meaning that the bias of $N_{CCN,AR\text{-}ave}$ is lower than 10% in most cases. It can be seen from the contour plot that large minus biases, ranging from -0.1 to -0.3, are all located between 12:00 and 18:00 LT. The large minus biases are caused by the increase of CCN activity, resulted from the increase of sulfate mass fraction in NPF event as discussed in section 3.2.1. Therefore, it can be concluded that in the NCP, the bias of N_{CCN} calculated with an average activation ratio may vary between 0 to 30%, depending on the type of the NPF events; while the bias is mainly within 10% in daytime in non-NPF days. It should be noted that this conclusion is based on "using an average activation ratio curve which is representative of the period and area studied". Using an inappropriate activation ratio curve (e.g. an average for another season or another region) may result in higher bias in calculated N_{CCN}.

The frequency distribution of the relative difference between $N_{CCN,D\text{-}ave}$ calculated with the average critical diameter and $N_{CCN,ref}$ is shown in fig. 7B. It can be seen that the overall frequency distribution is broader than that of $N_{CCN,AR\text{-}ave}$ but the majority of samples still locates between -0.1 and 0.1. However, a long tail can be seen on the left side. The underestimation of N_{CCN} in NPF events is clearer in the contour plot: large body of samples locates at relative difference between -0.1 to -0.5 in the afternoon. Therefore, applying a fixed critical diameter in the calculation of N_{CCN} might result in an underestimation up to 50% in NPF events in the NCP. We should also note that the critical diameter used here is actually "the best estimation" which derived from the samples used in the test. Assuming an arbitrary critical diameter may result in even larger bias in the estimation of N_{CCN}.

It is also worth to note that in both fig. 7A and B, there are a group of samples locates at relative difference between 0.1 and 0.3 in the evening, meaning that the N_{CCN} calculated with the average activation curve or critical diameter may sometimes be overestimated by up to 30% in the evening. As discussed in previous sections, this overestimation is basically caused by the increase of (nearly) hydrophobic matters, mostly BC, in the nocturnal boundary layer. Although BC comes from local anthropogenic emission, such an increase in BC concentration in the evening is actually a regional phenomenon, which was also observed in other studies in the NCP (e.g. Ma et al., 2011; Cheng et al., 2009). In the NCP, due to the very dense population and the developing industry and agriculture, the villages and cities are densely distributed in the region. The BC emitted from residential area in the evening may diffuse to the area around and causes an increase of the regional background of BC concentration.

3.4 Discussion

During NPF events, nucleation creates a large number of particles. The contribution of the NPF to N_{CCN} is mainly determined by the consequent growth processes, i.e. coagulation and condensation which enlarge the particles to CCN size range. As discussed before, the chemical composition of particles might change during these processes. In other words,

Atmos. Chem. Phys. Discuss., doi:10.5194/acp-2016-23, 2016
Manuscript under review for journal Atmos. Chem. Phys.
Published: 25 January 2016

besides enlarging the particles to CCN size range, those processes might also modify the particle CCN activity in varying degrees, depending on cases.

Two case studies are shown in section 3.2.1 and 3.2.2, both include a NPF event defined by a pronounced "banana pattern" in the time series of PNSD. But the CCN activity of the newly formed particles was found to be largely different. Measurements of particle hygroscopicity and chemical composition suggest that the growth of the newly formed particles in daytime is respectively dominated by sulfate and OM in the two cases, which results in different levels of CCN activity. This means that in the NCP, the CCN activity of newly formed particles during NPF events might be largely different. For example, during the sulfate-dominant event on July 22nd, the activation ratio curve shows a steep shape with lower D50 than the campaign average in the afternoon; while during the OM-dominant event on July 24th, the activation ratio curve in the afternoon is basically similar as the campaign average. These are only two selected cases. There might be also cases dominated by sulfate even more than that for July 22nd, or dominated by OM more than that for July 24th, or cases in between. Unfortunately, it is impossible to get any clue of the event type from the evolution of PNSD which is basically the only way to define a NPF event. It thus might be difficult to find a simple parameterization of size-resolved CCN activity for NPF events in the NCP which is appropriate for all cases.

For accurate estimation of N_{CCN} during a NPF event, we should not only focus on the increase of particle number concentration in certain size ranges. The variation of particle CCN activity should be also taken into account. However, we can only get this information from direct measurement CCN activity, or measurements of hygroscopicity or chemical composition, which are all difficult to be widely applied. Therefore average activation ratio curve or even a fixed critical diameter were usually used when evaluating the contribution of NPF on N_{CCN} (e.g. Laaksonen et al., 2005; Kuang et al., 2009; Asmi et al., 2011; Peng et al., 2014). From the discussion in section 3.3 we learned that the bias of the estimated N_{CCN} ranges from about 0 to 30% in NPF event if a fixed activation ratio curve (best estimation, representative of the region and season) is used. Using a fixed critical diameter is likely to result in larger underestimation of N_{CCN}. The bias can be up to 50% during NPF events. In daytime without NPF, the bias of estimated N_{CCN} can be limited within 10% if either a proper fix activation ratio curve or critical diameter is used. As a conclusion, we suggest not using a fixed critical diameter in the prediction of N_{CCN} in NPF seasons. If real-time CCN activity data is not available, using a proper fixed activation ratio curve can be a compromising choice.

As an important source of aerosol particles, NPF is very likely to have a great contribution on the amount of CCN. Due to the complexity of the process and the inhomogeneous spatial distribution of nucleation and consequent growth, at least in the NCP this contribution has not been well addressed. Wehner et al. (2010) found that NPF might occur at higher altitudes in the residual layer. This means NPF might be even more important in CCN budget than we expected. More cases of NPF with measurements of particle chemical composition and microphysical properties are therefore needed to better address its role. It would be also interesting to have some vertically resolved CCN measurements.

Our measurements only cover a period of about one month. The average activation ratio is proved to be good enough in the estimate of CCN number concentration in non-NPF periods. It is therefore worth to have a long-term (i.e. longer than one

Atmos. Chem. Phys. Discuss., doi:10.5194/acp-2016-23, 2016
Manuscript under review for journal Atmos. Chem. Phys.
Published: 25 January 2016

year) measurements of size-resolved activation ratio to provide a precise parameterization of CCN activity in different season or airmass types which can be used to estimate CCN number concentration with lower uncertainty.

4 Conclusion

To study the variation of particle CCN activity during NPF events in the NCP, size-resolved activation ratio as well as other particle physical and chemical properties were measured in a regional station in the north NCP.

New particle formation events were observed in 10 days out of 28 days, in which clear growth of newly formed particles were found in 5 days. In different NPF events, the hygroscopicity of newly formed particles was found to be largely different, suggesting that the particle growth might be dominated by different species. Two NPF events were selected for case studies, in which sulfate and organic matters are respectively responsible for the growth of the newly formed particles. The size-resolved activation ratio curves during the sulfate-dominated NPF event show a steep shape with lower $D_{P,50}$ than the campaign average; while the activation ratio curves during the OM-dominated event are basically similar as the campaign average. This means that during NPF in the NCP, the CCN activity of newly formed particles might be largely different.

To see the influence of assuming a constant CCN activity in the calculation of N_{CCN} in the NCP, N_{CCN} was calculated with the campaign average activation ratio curve and critical diameter, and then compared with the reference values. The bias of the estimated N_{CCN} ranges from about 0 to 30% in NPF event if a fixed activation ratio curve is used. Using a fix critical diameter is likely to result in larger underestimation of N_{CCN}. The bias can be up to 50% during NPF events. In daytime without NPF, the bias of estimated N_{CCN} can be limited within 10% if either a proper fix activation ratio curve or critical diameter is used.

We can learn from this study that for the accurate estimation of N_{CCN} during NPF events, one should not only focus on the increase of particle number concentration in certain size ranges. The variation of CCN activity should be also taken into account. It might be difficult to find a simple parameterization of size-resolved CCN activity for NPF events in the NCP, since it may vary a lot from case to case. Without real-time CCN activity data, a proper fixed activation ratio curve or critical dimeter can be used to calculated N_{CCN} for non-NPF daytime. But large uncertainty might appear in the N_{CCN} for NPF event, especially in case of using a fixed critical diameter.

Acknowledgment

This work is supported by the National Science Foundation of China under Grant No. 41590872, the project Sino German Science Center No. GZ663, and the EU project BACCHUS No. 603445.

Atmos. Chem. Phys. Discuss., doi:10.5194/acp-2016-23, 2016
Manuscript under review for journal Atmos. Chem. Phys.
Published: 25 January 2016

Reference

Asmi, E., Kivekäs, N., Kerminen, V.-M., Komppula, M., Hyvärinen, A.-P., Hatakka, J., Viisanen, Y., and Lihavainen, H.: Secondary new particle formation in Northern Finland Pallas site between the years 2000 and 2010, Atmos. Chem. Phys., 11, 12959-12972, doi:10.5194/acp-11-12959-2011, 2011.

Birmili, W., Berresheim, H., Plass-Dülmer, C., Elste, T., Gilge, S., Wiedensohler, A., and Uhrner, U.: The Hohenpeissenberg aerosol formation experiment (HAFEX): a long-term study including size-resolved aerosol, H_2SO_4, OH, and monoterpenes measurements, Atmos. Chem. Phys., 3, 361-376, doi:10.5194/acp-3-361-2003, 2003.

Boy, M., Kulmala, M., Ruuskanen, T. M., Pihlatie, M., Reissell, A., Aalto, P. P., Keronen, P., Dal Maso, M., Hellen, H., Hakola, H., Jansson, R., Hanke, M., and Arnold, F.: Sulphuric acid closure and contribution to nucleation mode particle growth, Atmos. Chem. Phys., 5, 863-878, doi:10.5194/acp-5-863-2005, 2005.

Cavalli, F., Viana, M., Yttri, K. E., Genberg, J., and Putaud, J.-P.: Toward a standardised thermal-optical protocol for measuring atmospheric organic and elemental carbon: the EUSAAR protocol, Atmos. Meas. Tech., 3, 79-89, doi:10.5194/amt-3-79-2010, 2010.

Cheng, Y. F., Berghof, M., Garland, R. M., Wiedensohler, A., Wehner, B., Müller, T., Su, H., Zhang, Y. H., Achtert, P., Nowak, A., Pöschl, U., Zhu, T., Hu, M., and Zeng, L. M.: Influence of soot mixing state on aerosol light absorption and single scattering albedo during air mass aging at a polluted regional site in northeastern China, J. Geophys. Res., 114, D00G10, doi:10.1029/2008JD010883, 2009.

Deng, Z. Z., Zhao, C. S., Zhang, Q., Huang, M. Y., and Ma, X. C.: Statistical analysis of microphysical properties and the parameterization of effective radius of warm clouds in Beijing area, Atmos. Res., 93, 888–896, 2009.

Deng, Z. Z., Zhao, C. S., Ma, N., Liu, P. F., Ran, L., Xu, W. Y., Chen, J., Liang, Z., Liang, S., Huang, M. Y., Ma, X. C., Zhang, Q., Quan, J. N., Yan, P., Henning, S., Mildenberger, K., Sommerhage, E., Schäfer, M., Stratmann, F., and Wiedensohler, A.: Size-resolved and bulk activation properties of aerosols in the North China Plain, Atmos. Chem. Phys., 11, 3835-3846, doi:10.5194/acp-11-3835-2011, 2011.

Deng, Z. Z., Zhao, C. S., Ma, N., Ran, L., Zhou, G. Q., Lu, D. R., and Zhou, X. J.: An examination of parameterizations for the CCN number concentration based on in situ measurements of aerosol activation properties in the North China Plain, Atmos. Chem. Phys., 13, 6227-6237, doi:10.5194/acp-13-6227-2013, 2013.

Dusek, U., Frank, G. P., Hildebrandt, L., Curtius, J., Schneider, J., Walter, S., Chand, D., Drewnick, F., Hings, S., Jung, D., Borrmann, S., and Andreae, M. O.: Size matters more than chemistry for cloud-nucleating ability of aerosol particles, Science, 312(5778), 1375–1378, 2006.

Ehn, M., Thornton, J. A., Kleist, E., Sipila, M., Junninen, H., Pullinen, I., Springer, M., Rubach, F., Tillmann, R., Lee, B., LopezHilfiker, F., Andres, S., Acir, I.-H., Rissanen, M., Jokinen, T., Schobesberger, S., Kangasluoma, J., Kontkanen, J., Nieminen, T., Kurten, T., Nielsen, L. B., Jorgensen, S., Kjaergaard, H. G., Canagaratna, M., Maso, M. D., Berndt,

T., Petaja, T., Wahner, A., Kerminen, V.-M., Kulmala, M., Worsnop, D. R., Wildt, J., and Mentel, T. F.: A large source of low-volatility secondary organic aerosol, Nature, 506, 476–479, 2014.

Guo, S., Hu, M., Zamora, M. L., Peng, J., Shang, D., Zheng, J., Du, Z., Wu, Z., Shao, M., and Zeng, L.: Elucidating severe urban haze formation in China, P. Natl. Acad. Sci. USA, 111, 17373–17378, 2014.

Gysel, M., McFiggans, G. B., and Coe, H.: Inversion of tandem differential mobility analyzer (TDMA) measurements, J. Aerosol Sci., 40, 134–151, doi:10.1016/j.jaerosci.2008.07.013, 2009.

Hagen, D. E. and Alofs, D. J.: Linear inversion method to obtain aerosol size distributions from measurements with a differential mobility analyzer, Aerosol Sci. Technol., 2, 465–475, 1983.

Kecorius, S., Zhang, S., Wang, Z., Größ, J., Ma, N., Wu, Z., Ran, L., Hu, M., Wang, P., Ulevičius, V., and Wiedensohler, A.: Nocturnal aerosol particle formation in the North China Plain, Lith. J. Phys., 55, 44–53, 2015.

Kerminen, V.-M., Virkkula, A., Hillamo, R., Wexler, A. S., and Kulmala, M.: Secondary organics and atmospheric cloud condensation nuclei production, J. Geophys. Res., 105, 9255–9264, 2000.

Kerminen, V.-M., Paramonov, M., Anttila, T., Riipinen, I., Fountoukis, C., Korhonen, H., Asmi, E., Laakso, L., Lihavainen, H., Swietlicki, E., Svenningsson, B., Asmi, A., Pandis, S. N., Kulmala, M., and Petäjä, T.: Cloud condensation nuclei production associated with atmospheric nucleation: a synthesis based on existing literature and new results, Atmos. Chem. Phys., 12, 12037-12059, doi:10.5194/acp-12-12037-2012, 2012.

Kuang, C., McMurry, P., and McCormick, A.: Determination of cloud condensation nuclei production from measured new particle formation events, Geophys. Res. Lett., 36, L09822, doi:10.1029/2007JD009253, 2009.

Kulmala, M., Toivonen, A., Mäkelä, J. M., and Laaksonen, A.: Analysis of the growth of nucleation mode particles observed in Boreal forest, Tellus, 50B, 449–462, 1998.

Kulmala, M., Dal Maso, M., Mäkelä, J. M., Pirjola, L., Väkevä, M., Aalto, P., Miikkulainen, P., Hämeri, K., and O'Dowd, C. D.: On the formation, growth and composition of nucleation mode particles, Tellus, 53B, 479–490, 2001.

Kulmala, M., Vehkamäki, H., Petäjä, T., Dal Maso, M., Lauri, A., Kerminen, V.-M., Birmili, W., and McMurry, P. H.: Formation and growth rates of ultrafine atmospheric particles: A review of observations, J. Aerosol Sci., 35, 143–176, 2004.

Kulmala, M., Riipinen, I., Sipilä, M., Manninen, H. E., Petäjä, T., Junninen, H., Dal Maso, M., Mordas, G., Mirme, A., Vana, M., Hirsikko, A., Laakso, L., Harrison, R. M., Hanson, I., Leung, C., Lehtinen, K. E. J., and Kerminen, V.-M.: Towards Direct Measurement of Atmospheric Nucleation, Science, 318, 89–92, 2007.

Kulmala, M. and Kerminen, V.-M.: On the formation and growth of atmospheric nanoparticles, Atmos. Res., 90, 132–150, doi:10.1016/j.atmosres.2008.01.005, 2008.

Kuwata, M., Kondo, Y., Miyazaki, Y., Komazaki, Y., Kim, J. H., Yum, S. S., Tanimoto, H., and Matsueda, H.: Cloud condensation nuclei activity at Jeju Island, Korea in spring 2005, Atmos. Chem. Phys., 8, 2933-2948, doi:10.5194/acp-8-2933-2008, 2008.

Laaksonen, A., Hamed, A., Joutsensaari, J., Hiltunen, L., Cavalli, F., Junkermann, W., Asmi, A., Fuzzi, S., and Faccini, M. C.: Cloud condensation nucleus production from nucleation events at a highly polluted region, Geophys. Res. Lett., 32, L06812, doi:10.1029/2004GL022092, 2005.

Laaksonen, A., Kulmala, M., O'Dowd, C. D., Joutsensaari, J., Vaattovaara, P., Mikkonen, S., Lehtinen, K. E. J., Sogacheva, L., Dal Maso, M., Aalto, P., Petäjä, T., Sogachev, A., Yoon, Y. J., Lihavainen, H., Nilsson, D., Facchini, M. C., Cavalli, F., Fuzzi, S., Hoffmann, T., Arnold, F., Hanke, M., Sellegri, K., Umann, B., Junkermann, W., Coe, H., Allan, J. D., Alfarra, M. R., Worsnop, D. R., Riekkola, M. -L., Hyötyläinen, T., and Viisanen, Y.: The role of VOC oxidation products in continental new particle formation, Atmos. Chem. Phys., 8, 2657-2665, doi:10.5194/acp-8-2657-2008, 2008.

Lance, S., Medina, J., Smith, J. N., and Nenes, A.: Mapping the operation of the DMT Continuous Flow CCN counter, Aerosol Sci. Technol., 40, 242–254, 2006.

Liu, P. F., Zhao, C. S., Göbel, T., Hallbauer, E., Nowak, A., Ran, L., Xu, W. Y., Deng, Z. Z., Ma, N., Mildenberger, K., Henning, S., Stratmann, F., and Wiedensohler, A.: Hygroscopic properties of aerosol particles at high relative humidity and their diurnal variations in the North China Plain, Atmos. Chem. Phys., 11, 3479-3494, doi:10.5194/acp-11-3479-2011, 2011.

Ma, N., Zhao, C. S., Nowak, A., Müller, T., Pfeifer, S., Cheng, Y. F., Deng, Z.Z., Liu, P. F., Xu, W. Y., Ran, L., Yan, P., Göbel, T., Hallbauer, E., Mildenberger, K., Henning, S., Yu, J., Chen, L. L., Zhou, X. J., Stratmann, F., and Wiedensohler, A.: Aerosol optical properties in the North China Plain during HaChi campaign: an in-situ optical closure study, Atmos. Chem. Phys., 11, 5959-5973, doi:10.5194/acp-11-5959-2011, 2011.

Ma, N., Zhao, C. S., Müller, T., Cheng, Y. F., Liu, P. F., Deng, Z. Z., Xu, W. Y., Ran, L., Nekat, B., van Pinxteren, D., Gnauk, T., Müller, K., Herrmann, H., Yan, P., Zhou, X. J., and Wiedensohler, A.: A new method to determine the mixing state of light absorbing carbonaceous using the measured aerosol optical properties and number size distributions, Atmos. Chem. Phys., 12, 2381-2397, doi:10.5194/acp-12-2381-2012, 2012.

Massling, A., Leinert, S., Wiedensohler, A., and Covert, D.: Hygroscopic growth of sub-micrometer and one-micrometer aerosol particles measured during ACE-Asia, Atmos. Chem. Phys., 7, 3249-3259, doi:10.5194/acp-7-3249-2007, 2007.

Peng, J. F., Hu, M., Wang, Z. B., Huang, X. F., Kumar, P., Wu, Z. J., Guo, S., Yue, D. L., Shang, D. J., Zheng, Z., and He, L. Y.: Submicron aerosols at thirteen diversified sites in China: size distribution, new particle formation and corresponding contribution to cloud condensation nuclei production, Atmos. Chem. Phys., 14, 10249-10265, doi:10.5194/acp-14-10249-2014, 2014.

Petters, M. D. and Kreidenweis, S. M.: A single parameter representation of hygroscopic growth and cloud condensation nucleus activity, Atmos. Chem. Phys., 7, 1961-1971, doi:10.5194/acp-7-1961-2007, 2007.

Pfeifer, S., Birmili, W., Schladitz, A., Müller, T., Nowak, A., and Wiedensohler, A.: A fast and easy-to-implement inversion algorithm for mobility particle size spectrometers considering particle number size distribution information outside of the detection range, Atmos. Meas. Tech., 7, 95-105, doi:10.5194/amt-7-95-2014, 2014.

Roberts, G. C. and Nenes, A.: A continuous-flow streamwise thermal-gradient CCN chamber for atmospheric measurements, Aerosol Sci. Technol., 39, 206–221, 2005.

Rose, D., Gunthe, S. S., Mikhailov, E., Frank, G. P., Dusek, U., Andreae, M. O., and Pöschl, U.: Calibration and measurement uncertainties of a continuous-flow cloud condensation nuclei counter (DMT-CCNC): CCN activation of ammonium sulfate and sodium chloride aerosol particles in theory and experiment, Atmos. Chem. Phys., 8, 1153-1179, doi:10.5194/acp-8-1153-2008, 2008.

Shen, X. J., Sun, J. Y., Zhang, Y. M., Wehner, B., Nowak, A., Tuch, T., Zhang, X. C., Wang, T. T., Zhou, H. G., Zhang, X. L., Dong, F., Birmili, W., and Wiedensohler, A.: First long-term study of particle number size distributions and new particle formation events of regional aerosol in the North China Plain, Atmos. Chem. Phys., 11, 1565-1580, doi:10.5194/acp-11-1565-2011, 2011.

Sihto, S.-L., Mikkilä, J., Vanhanen, J., Ehn, M., Liao, L., Lehtipalo, K., Aalto, P. P., Duplissy, J., Petäjä, T., Kerminen, V.-M., Boy, M., and Kulmala, M.: Seasonal variation of CCN concentrations and aerosol activation properties in boreal forest, Atmos. Chem. Phys., 11, 13269-13285, doi:10.5194/acp-11-13269-2011, 2011.

Smith, J. N., Barsanti, K. C., Friedl, H. R., Ehn, M., Kulmala, M., Collins, D. R., Scheckman, J. H., Williams, B. J., and McMurry, P. H.: Observations of aminium salts in atmospheric nanoparticles and possible climatic implications, P. Natl. Acad. Sci. USA, 107, 6634– 6639, 2010.

Su, H., Rose, D., Cheng, Y. F., Gunthe, S. S., Massling, A., Stock, M., Wiedensohler, A., Andreae, M. O., and Pöschl, U.: Hygroscopicity distribution concept for measurement data analysis and modeling of aerosol particle mixing state with regard to hygroscopic growth and CCN activation, Atmos. Chem. Phys., 10, 7489-7503, doi:10.5194/acp-10-7489-2010, 2010.

Tuch, T. M., Haudek, A., Müller, T., Nowak, A., Wex, H., and Wiedensohler, A.: Design and performance of an automatic regenerating adsorption aerosol dryer for continuous operation at monitoring sites, Atmos. Meas. Tech., 2, 417-422, doi:10.5194/amt-2-417-2009, 2009.

Wang, Z. B., Hu, M., Wu, Z. J., and Yue, D. L., Reaserch on the formation mechanism of new particles in the atmosphere, Acta Chim. Sinica, 71, 519–527, 2013a.

Wang, Z. B., Hu, M., Sun, J. Y., Wu, Z. J., Yue, D. L., Shen, X. J., Zhang, Y. M., Pei, X. Y., Cheng, Y. F., and Wiedensohler, A.: Characteristics of regional new particle formation in urban and regional background environments in the North China Plain, Atmos. Chem. Phys., 13, 12495-12506, doi:10.5194/acp-13-12495-2013, 2013b.

Wehner, B., Petäjä, T., Boy, M., Engler, C., Birmili, W., Tuch, T., Wiedensohler, A., and Kulmala, M.: The contribution of sulfuric acid and non-volatile compounds on the growth of freshly formed atmospheric aerosols, Geophys. Res. Lett., 32, L17810, doi:10.1029/2005gl023827, 2005.

Wehner, B., Berghof, M., Cheng, Y. F., Achtert, P., Birmili, W., Nowak, A., Wiedensohler, A., Garland, R. M., Pöschl, U., Hu, M., and Zhu, T.: Mixing state of nonvolatile aerosol particle fractions and comparison with light absorption in the polluted Beijing region, J. Geophys. Res., 114, D00G17, doi:10.1029/2008JD010923, 2009.

Wiedensohler, A., Orsini, D., Covert, D. S., Coffmann, D., Cantrell, W., Havlicek, M., Brechtel, F. J., Russell, L. M., Weber, R. J., Gras, J., Hudson, J. G., Litchy, M.: Intercomparsion study of the size-dependent counting efficiency of 26 condensation particle counters, Aerosol Sci. Technol., 27, 224–242, 1997.

Wiedensohler, A., Cheng, Y. F., Nowak, A., Wehner, B., Achtert, P., Berghof, M., Birmili, W., Wu, Z. J., Hu, M., Zhu, T., Takegawa, N., Kita, K., Kondo, Y., Lou, S. R., Hofzumahaus, A., Holland, F., Wahner, A., Gunthe, S. S., Rose, D., Su, H., and Poschl, U.: Rapid aerosol particle growth and increase of cloud condensation nucleus activity by secondary aerosol formation and condensation: A case study for regional air pollution in northeastern China, J. Geophys. Res., 114, D00G08, doi:10.1029/2008JD0101884, 2009.

Wiedensohler, A., Birmili, W., Nowak, A., Sonntag, A., Weinhold, K., Merkel, M., Wehner, B., Tuch, T., Pfeifer, S., Fiebig, M., Fjaraa, A. M., Asmi, E., Sellegri, K., Depuy, R., Venzac, H., Villani, P., Laj, P., Aalto, P., Ogren, J. A., Swietlicki, E., Williams, P., Roldin, P., Quincey, P., Huglin, C., Fierz-Schmidhauser, R., Gysel, M., Weingartner, E., Riccobono, F., Santos, S., Gruning, C., Faloon, K., Beddows, D., Harrison, R., Monahan, C., Jennings, S. G., O'Dowd, C. D., Marinoni, A., Horn, H. G., Keck, L., Jiang, J., Scheckman, J., McMurry, P. H., Deng, Z., Zhao, C. S., Moerman, M., Henzing, B., de Leeuw, G., Loschau, G., and Bastian, S.: Mobility particle size spectrometers: harmonization of technical standards and data structure to facilitate high quality long-term observations of atmospheric particle number size distributions, Atmos. Meas. Tech., 5, 657–685, doi:10.5194/amt- 5-657-2012, 2012.

Wiedensohler, A., Birmili, W., Putaud, J. P., and Ogren, J.: Recommendations for Aerosol Sampling, Aerosol Science: Technology and Applications, John Wiley & Sons, Ltd, 45-59, 2013.

Wu, Z., Hu, M., Liu, S., Wehner, B., Bauer, S., Maßling, A., Wiedensohler, A., Petäjä, T., Dal Maso, M., Kulmala, M.: New particle formation in Beijing, China: Statistical analysis of a 1-year data set, J. Geophys. Res., 112, D09209, doi:10.1029/2006JD007406, 2007.

Wu, Z. J., Poulain, L., Birmili, W., Größ, J., Niedermeier, N., Wang, Z. B., Herrmann, H., and Wiedensohler, A.: Some insights into the condensing vapors driving new particle growth to CCN sizes on the basis of hygroscopicity measurements, Atmos. Chem. Phys., 15, 13071-13083, doi:10.5194/acp-15-13071-2015, 2015.

Xu, W. Y., Zhao, C. S., Ran, L., Deng, Z. Z., Liu, P. F., Ma, N., Lin, W. L., Xu, X. B., Yan, P., He, X., Yu, J., Liang, W. D., and Chen, L. L.: Characteristics of pollutants and their correlation to meteorological conditions at a suburban site in the North China Plain, Atmos. Chem. Phys., 11, 4353-4369, doi:10.5194/acp-11-4353-2011, 2011.

Yue, D. L., Hu, M., Zhang, R. Y., Wang, Z. B., Zheng, J., Wu, Z. J., Wiedensohler, A., He, L. Y., Huang, X. F., and Zhu, T.: The roles of sulfuric acid in new particle formation and growth in the mega-city of Beijing, Atmos. Chem. Phys., 10, 4953-4960, doi:10.5194/acp-10-4953-2010, 2010.

Yue, D. L., Hu, M., Zhang, R. Y., Wu, Z. J., Su, H., Wang, Z. B., Peng, J. F., He, L. Y., Huang, X. F., Gong, Y. G., and Wiedensohler, A.: Potential contribution of new particle formation to cloud condensation nuclei in Beijing, Atmos. Environ., 45, 6070–6077, 2011.

Zhang, S. L., Ma, N., Kecorius, S., Wang, P. C., Hu, M., Wang, Z. B., Größ, J., Wu, Z. J., and Wiedensohler, A.: Mixing state of atmospheric particles over the North China Plain, Atmos. Environ., 125, 152-164, 2016.

Zhao, C., Tie, X., Brasseur, G., Noone, K. J., Nakajima, T., Zhang, Q., Zhang, R., Huang, M., Duan, Y., Li, G., and Ishizaka, Y.: Aircraft measurements of cloud droplet spectral dispersion and implications for indirect aerosol radiative forcing, Geophys. Res. Lett., 33, L16809, doi:10.1029/2006gl026653, 2006a.

Zhao, C., Tie, X., and Lin, Y.: A possible positive feedback of reduction of precipitation and increase in aerosols over Eastern Central China, Geophys. Res. Lett., 33, L11814, doi:10.1029/2006gl025959, 2006b.

Atmos. Chem. Phys. Discuss., doi:10.5194/acp-2016-23, 2016
Manuscript under review for journal Atmos. Chem. Phys.
Published: 25 January 2016

Figure 1: Map of the NCP. The observational site is marked as a red point. Urban areas are marked in yellow. The green line denotes the contour line of 500 m a.s.l., which can be considered as the natural boundary of the NCP.

Atmos. Chem. Phys. Discuss., doi:10.5194/acp-2016-23, 2016
Manuscript under review for journal Atmos. Chem. Phys.
Published: 25 January 2016

Atmospheric Chemistry and Physics Discussions

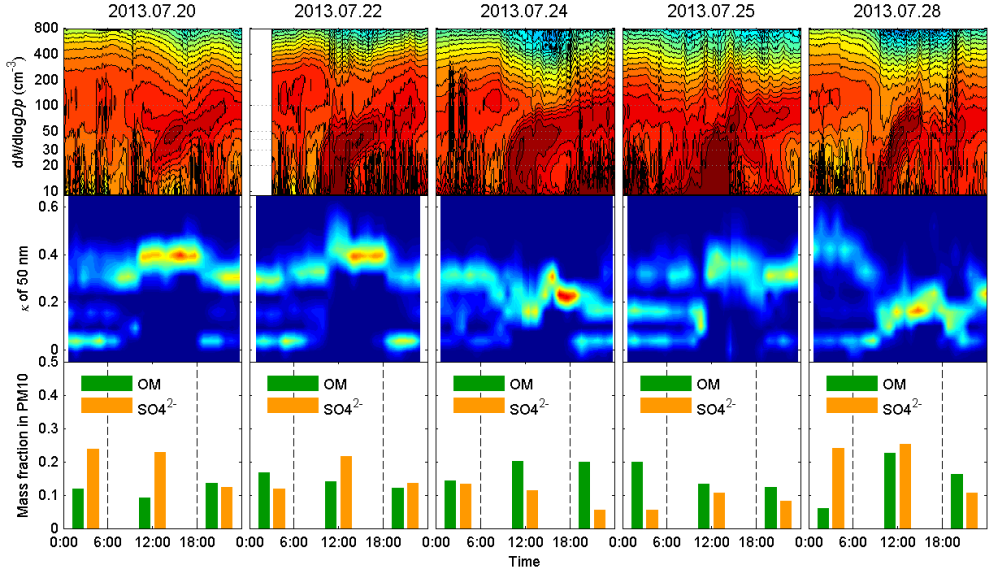

Figure 2. 5 NPF events observed during the campaign period. Subplots show the time series of particles number size distribution (upper), κ-PDF of 50 nm particles (middle), and mass fraction of organic matters and sulfate from PM10 HV-sample analysis (lower).

5

Atmos. Chem. Phys. Discuss., doi:10.5194/acp-2016-23, 2016
Manuscript under review for journal Atmos. Chem. Phys.
Published: 25 January 2016

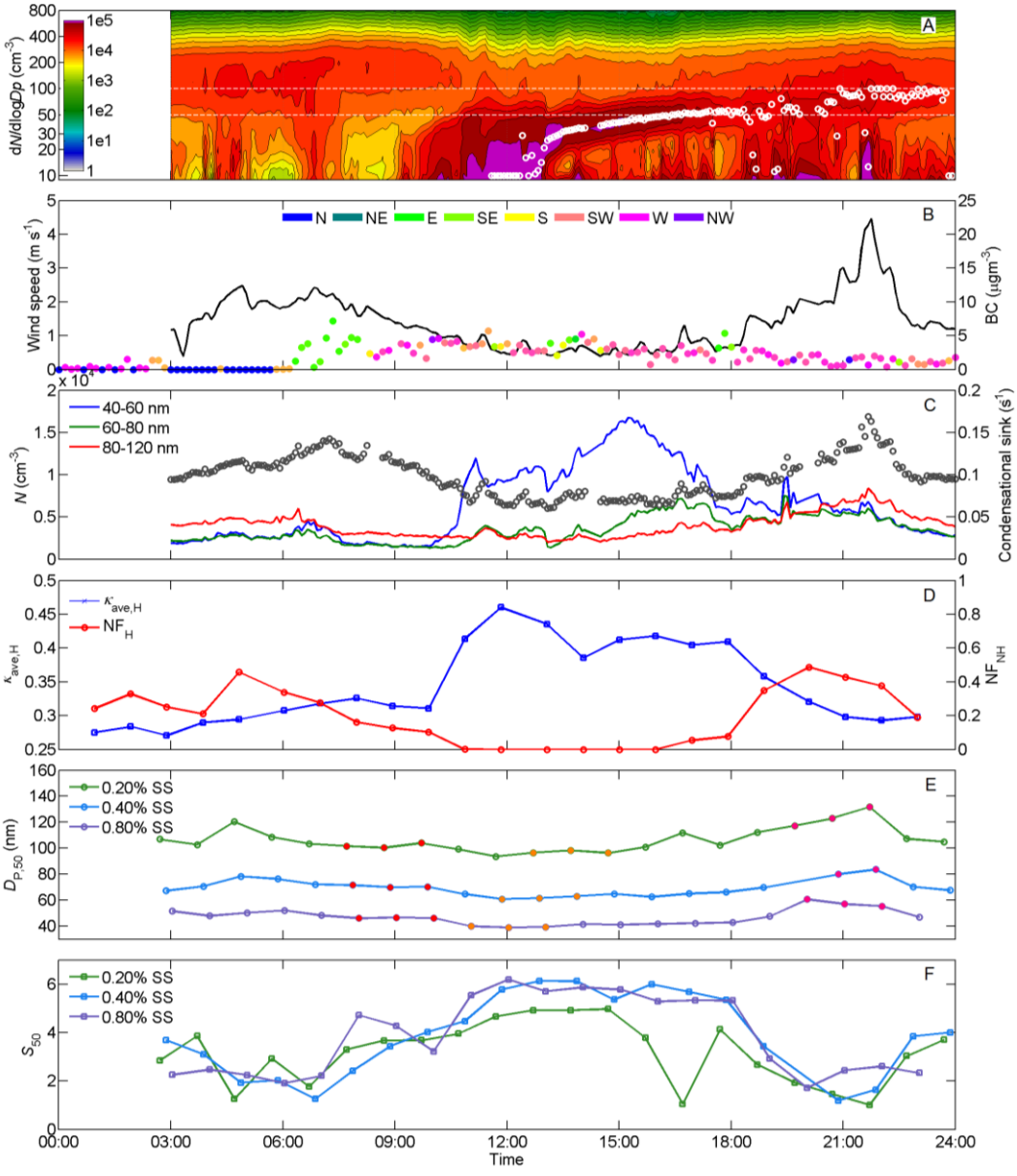

Figure 3. Time series of particle number size distribution and geometric mean diameter of nucleation mode (A), wind speed/direction and BC mass concentration (B), number concentration of particles in defined size ranges and condensational sink (C), average κ of hygroscopic mode and number fraction of hydrophobic mode for 50 nm particles (D), $D_{P,50}$ for 0.20%, 0.40% and 0.80% SS (E), as well as S_{50} for the three SS (F) on July 22nd. Points filled with color in subplot E show the records selected to calculate the average size-resolved activation ratio shown in Figure 5.

Atmos. Chem. Phys. Discuss., doi:10.5194/acp-2016-23, 2016
Manuscript under review for journal Atmos. Chem. Phys.
Published: 25 January 2016

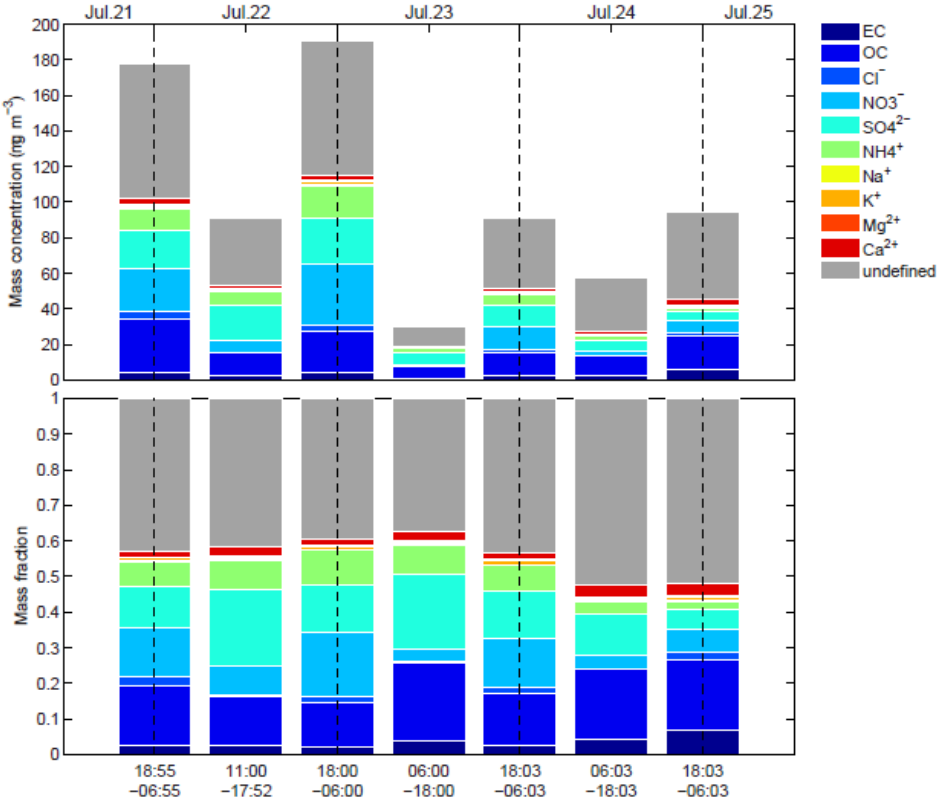

Figure 4. Mass concentration and mass fraction of chemical compounds in PM10 during the two NPF events

Atmos. Chem. Phys. Discuss., doi:10.5194/acp-2016-23, 2016
Manuscript under review for journal Atmos. Chem. Phys.
Published: 25 January 2016

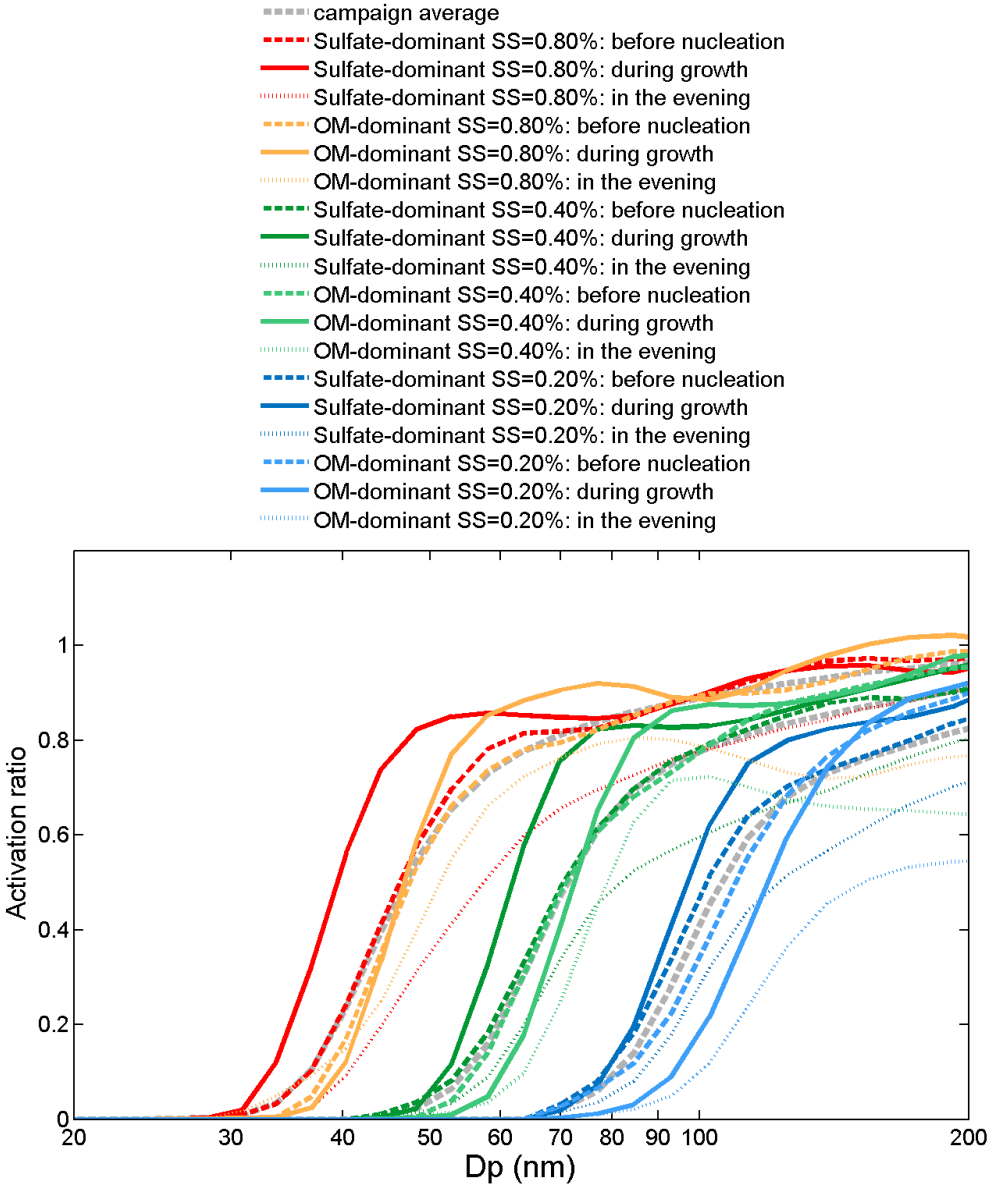

Figure 5. Average size-resolved activation ratio for the selected periods on July 22nd and 24th

Atmos. Chem. Phys. Discuss., doi:10.5194/acp-2016-23, 2016
Manuscript under review for journal Atmos. Chem. Phys.
Published: 25 January 2016

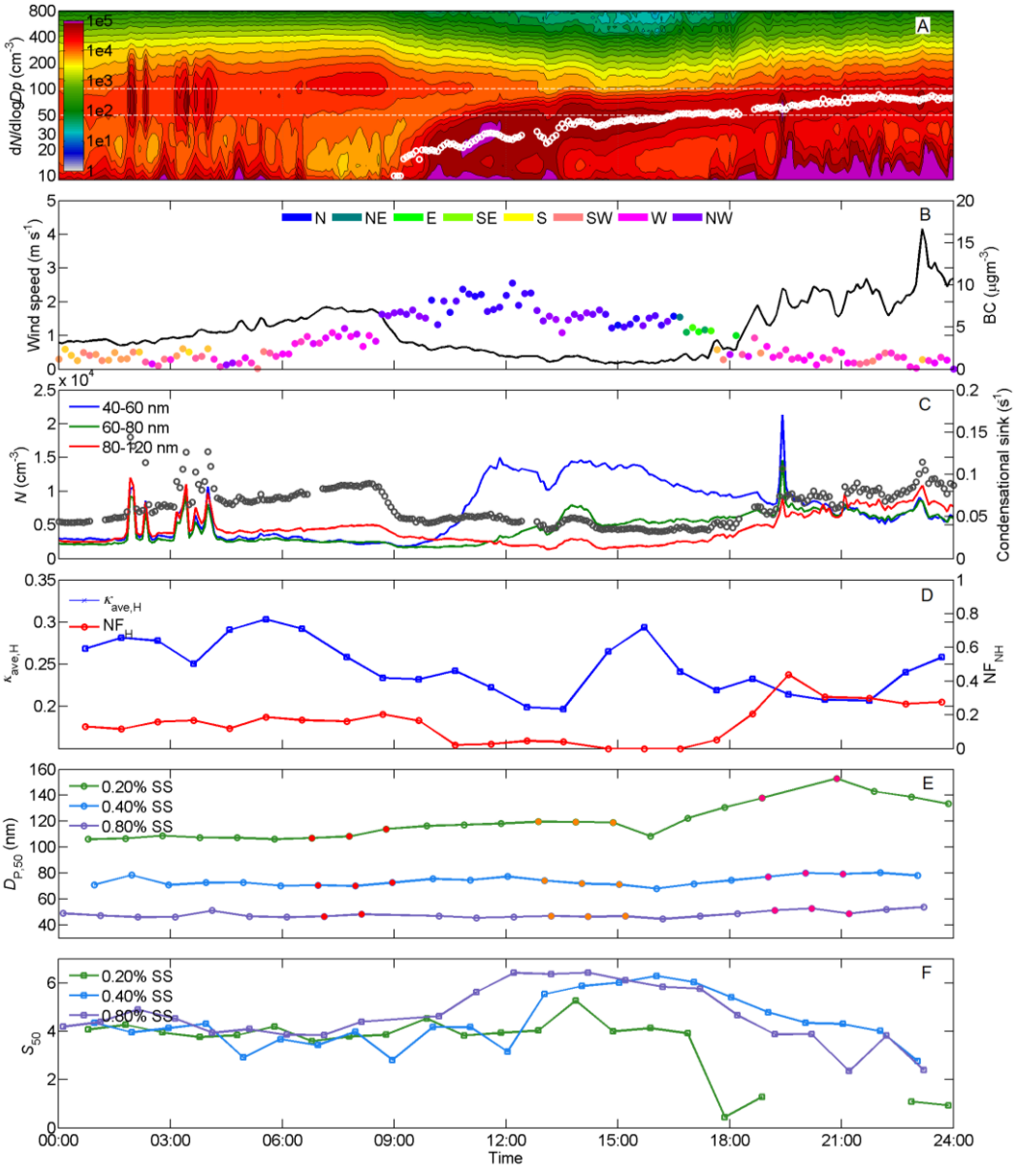

Figure 6. Time series of particle number size distribution and geometric mean diameter of nucleation mode (A), wind speed/direction and BC mass concentration (B), number concentration of particles in defined size ranges and condensational sink (C), average κ of hygroscopic mode and number fraction of hydrophobic mode for 50 nm particles (D), $D_{P,50}$ for 0.20%, 0.40% and 0.80% SS (E), as well as S_{50} for the three SS (F) on July 24th. Points filled with color in subplot E show the records selected to calculate the average size-resolved activation ratio shown in Figure 5.

Atmos. Chem. Phys. Discuss., doi:10.5194/acp-2016-23, 2016
Manuscript under review for journal Atmos. Chem. Phys.
Published: 25 January 2016

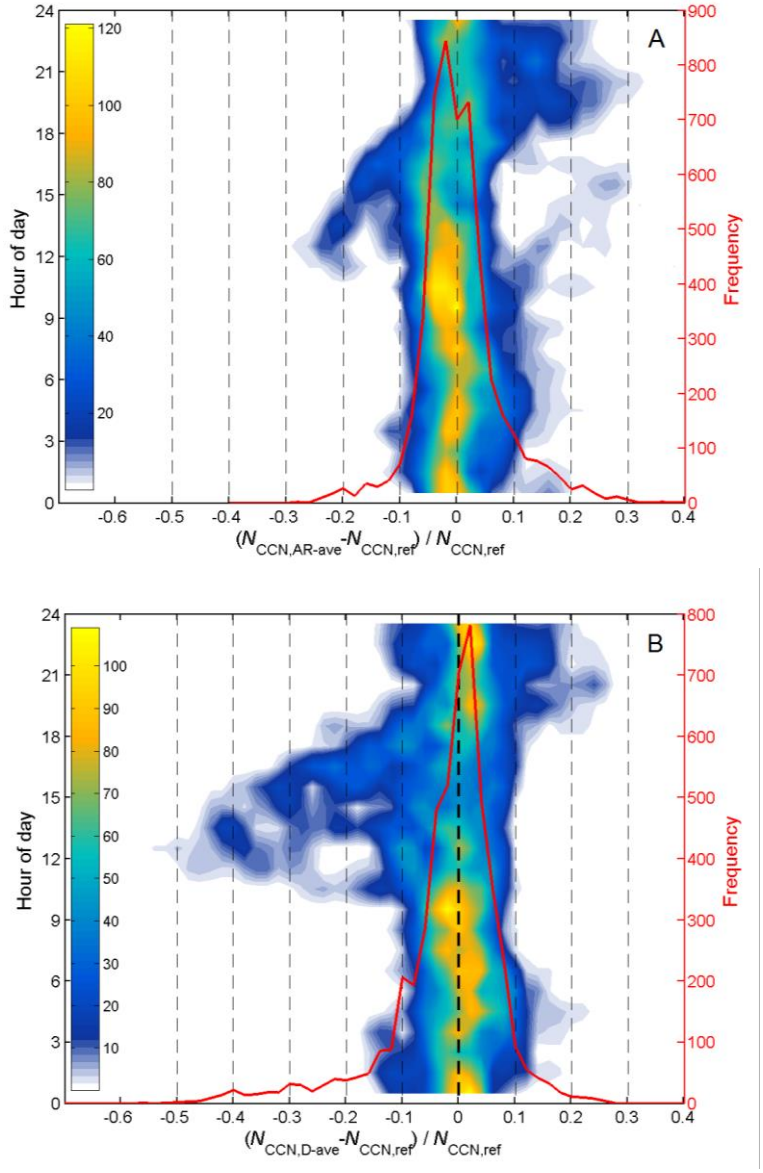

Figure 7. Frequency distribution at different time of day and overall frequency distribution of the relative difference between $N_{CCN\text{-}ave}$ and $N_{CCN\text{-}real}$, and between $N_{CCN\text{-}Dcri}$ and $N_{CCN\text{-}real}$